JOURNAL OF Materials CHEMISTRY

High-order stimulated Raman scattering in a $\chi^{(3)}$-active molecular glass: $Ca(NO_3)_2:KNO_3$ under picosecond excitation

René Burkhalter,[a] Bernhard Trusch,[a] Patrick Franz,[a] Alexander A. Kaminskii,[b] Hans J. Eichler[c] and Jürg Hulliger*[a]

[a]*Department of Chemistry and Biochemistry, University of Berne, Freiestrasse 3, CH-3012 Berne, Switzerland. E-mail: juerg.hulliger@iac.unibe.ch; Fax: +41 31 631 39 93; Tel: +41 31 631 42 41*

[b]*Institute of Crystallography, Russian Academy of Sciences, Leninsky prospekt 59, 117333 Moscow, Russia*

[c]*Optical Institute, Technical University of Berlin, Strasse des 17. Juni 135, D-10623 Berlin, Germany*

Received 28th March 2001, Accepted 17th September 2001
First published as an Advance Article on the web 9th October 2001

The preparation of crack-free $Ca(NO_3)_2:KNO_3$ glass samples several centimeters long contained in cuvettes is reported. The mechanical stability of nitrate glasses was improved by adding oxide glass fibers, along with partial tuning of the indices of refraction by addition of Cd^{2+} ions. Efficient $\chi^{(3)}$ frequency conversion processes leading to multicolour emission in the visible region down to 0.4555 μm and near-infrared range are due to multiple anti-Stokes and Stokes shifts observed for 10 mm long $Ca(NO_3)_2:KNO_3$ and $Ca(NO_3)_2:Cd(NO_3)_2:KNO_3$ samples under picosecond excitation. All laser scattering components were identified and attributed to the SRS-active vibration mode $\omega_{SRS}=1049$–$1053\ cm^{-1}$ of the molecular $[NO_3]^-$ ions.

1 Introduction

Stimulated Raman scattering (SRS) in solids can give rise to intense Stokes and anti-Stokes-shifted optical frequencies if the molecular vibrations of highly polarisable bonds contribute to the $\chi^{(3)}$ of a material. Attractive SRS gain coefficients can be obtained for materials featuring a large third-order nonlinear susceptibility. Multiple Stokes ($\omega_f > \omega_{St}$) and anti-Stokes ($\omega_f < \omega_{ASt}$) shifts ranging from ~90 to ~3100 cm^{-1} are known for SRS[1–4] in various bulk materials, including inorganic salt crystals such as niobates,[5] iodates,[6] nitrates,[7,8] tungstates and molybdates,[9–11] sulfates,[12] chlorates,[13] borates,[14,15] fluorides[16] *etc.* Nanosecond and picosecond Raman lasers built on the basis of bulk single crystals are known for α-$LiIO_3$,[6] HIO_3,[17] $Ba(NO_3)_2$,[18,19] α-$KGd(WO_4)_2$,[20,21] $NaBrO_3$,[22] $CaWO_4$,[23] $PbWO_4$,[24] *etc.*, and for P_2O_5 or GeO_2-doped glass fibers.[25–28] At present, some of them have already been commercialised.[29–31] Given a $\chi^{(3)}$ effect, a high input power and a typical interaction length of several centimeters are necessary. In this respect, glasses of the corresponding crystalline materials are promising SRS media for new laser applications, including fibers. In the course of our recent study on $Sr(NO_3)_2$ and $CsNO_3$ (phase II) single crystals, which showed high efficient Stokes and anti-Stokes generation,[8] (and also taking into account numerous SRS data on cubic $Ba(NO_3)_2$ [7,8,18,19]) we have investigated nitrate glasses as possible $\chi^{(3)}$-active media for Raman laser shifters.

Nitrate glasses were discovered by Rostkowsky in 1930.[32] Thilo *et al.* have investigated the stability range of the glassy region of binary nitrate systems.[33] Vinogradow *et al.* showed later that ternary nitrate mixtures can also form glasses. Ternary glasses can be doped with rare earth elements, which show strong luminescence upon excitation in the UV.[34] Nitrate glasses in general have been widely used as a model for glassy systems.[35] To the best of our knowledge, no SRS studies on nitrate glasses have been published previously.

2 $Ca(NO_3)_2:KNO_3$ glass preparation

Due to the high hygroscopicity of nitrate glasses, we had to prepare samples within cuvettes, in order to circumvent the polishing of end faces. Pure CKN [$Ca(NO_3)_2:KNO_3=40:60$, mol%] glass shows only a slight tendency to crystallisation when cooling to room temperature occurs rapidly, although this couldn't be confirmed by DSC measurements. Initial attempts to fill the cuvettes revealed that, due to the large difference in the expansion coefficients of Pyrex and the nitrate glass, samples showed cracking (as did the cuvettes on occasion). Therefore, slow cooling rates were applied, however, cooling rates lower than 10 °C h^{-1} always led to crystallisation of the nitrate melt. To prevent nucleation, we tested ingredients obtained from various inorganic salts and some organic materials—so far without success.

To avoid cracking, we finally applied a cooling rate of about 10 to 20 °C h^{-1}. Glasses of the composition: $Ca(NO_3)_2:KNO_3=40:60$ (mol%) were prepared from $Ca(NO_3)_2{\cdot}4H_2O$ (Fluka, puriss p.a.) and KNO_3 (Merck, p.a.). Starting materials were placed in an oxide glass container and heated to 240 °C for 1.5 h in air to remove water. Thereafter, fast cooling down to 120 °C was applied and samples were kept at this temperature for 45 min. As described, clear and crack-free samples were occasionally obtained. However, these materials turned out to be full of mechanical stress. Exposure to small temperature gradients (5 to 10 °C) led to cracking of both the sample and the container. To reduce the interaction between the nitrate glass and the container, cuvettes were treated with silicon fluid. A 0.4 wt% solution of silicon fluid (Dow Corning 200/200 cs) in toluene was prepared and the containers filled with it. The solution was kept in the containers at 60 °C for about an hour. After removal of the silicon fluid solution, the containers were heated to 350 °C for 2 to 3 h. Crack-free CKN [$Ca(NO_3)_2:KNO_3=40:60$, mol%] glass of 10 to 15 mm length could be obtained inside such containers.

DOI: 10.1039/b102841n

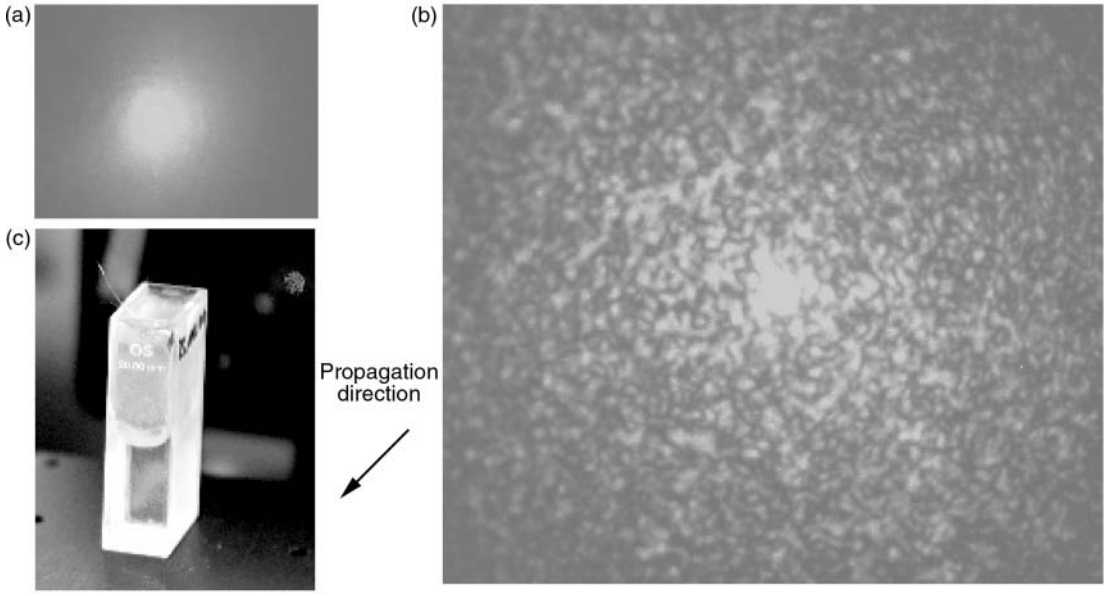

Fig. 1 Scattering properties of the composite nitrate glass: (a) He–Ne-laser beam passing through air; (b) He–Ne-laser beam after passing a 20 mm long cadmium-containing composite glass. Scattering is due to an imperfect match between the refractive indices of the nitrate glass and the oxide fibers; (c) Tyndall effect when a He–Ne laser beam passes through a cuvette of 20 mm in length.

With the idea of improving the mechanical stability of the glass, we incorporated oxide glass fibers milled to a length of 5 to 20 μm to obtain a composite material cross-linked by a stiff component. Immediately, it became clear that nitrate glasses containing fibers, could withstand cooling from 120 °C to room temperature within a few minutes without cracking. A new issue to be addressed at this point was that these fibers did not match the refractive index of the nitrate glass (oxide: $n_D = 1.52$, determined by the method of Becke;[36] CKN: $n_D > 1.50$). By adding $Cd(NO_3)_2$ to the CKN, we finally succeeded in raising the refractive index of the nitrate glass to about 1.52 [optimum composition: $Ca(NO_3)_2 : Cd(NO_3)_2 : KNO_3 = 29.11 : 15.62 : 55.27$, mol%], without promoting crystallisation. Unfortunately, perfect index matching ($\delta n < 10^{-4}$) has not, thus far, been achieved (Fig. 1). Glasses containing $Cd(NO_3)_2$ were held at 240 °C for 1.5 h, followed by immediate cooling to 100 °C, at which temperature they were kept for 45 min. The composite glass (1.7 wt% fibers) allowed us to fabricate 20 mm long crack-free ingots contained in cuvettes (Fig. 2). These samples were sealed with DEMOTEC 33 polymer to protect them against ambient moisture.

Varying the temperature may be another approach to matching the refractive indices of the fibers and the nitrate glass. No improvement in the scattering behaviour was observed within the temperature range 0-80 °C. Literature data on the temperature variation of the refractive index of CKN reports only small changes in δn of ~ 0.001 per 10 °C.[37] The present mismatch may well be of the order of $\delta n \cong 0.008$–0.01.

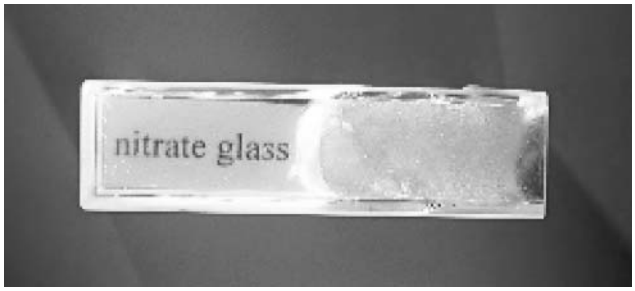

Fig. 2 Cuvette (20 mm long) filled with cadmium composite glass.

3 Raman and SRS experiments on $Ca(NO_3)_2 : KNO_3$ and composite glass samples

The measured spontaneous Raman scattering spectra for pure CKN and the composite glass (Fig. 3) agree well with data in ref. 38 The most intense line around 1050 cm^{-1} corresponds to undistorted $[NO_3]^-$ ions of symmetry D_{3h} and can be assigned to the N–O fundamental symmetric stretching mode ν_1 (A_1') found in nitrate melts.[38,39] For the excitation of a high-order Stokes and anti-Stokes single-pass generation in the $\chi^{(3)}$-active

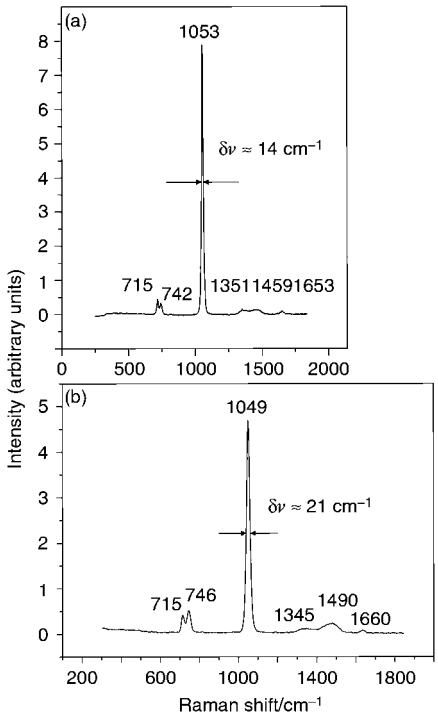

Fig. 3 Room temperature spontaneous Raman scattering spectra: (a) CKN glass [$Ca(NO_3)_2 : KNO_3 = 40 : 60$, mol%]. Zero corresponds to the He–Ne laser excitation at a wavelength of 0.6328 μm. (b) [$Ca(NO_3)_2 : Cd(NO_3)_2 : KNO_3 = 29.11 : 15.62 : 55.27$, mol%]. Zero corresponds to the Nd : YAG laser excitation at 1.0645 μm wavelength. The Raman shifts of all lines are given in cm^{-1}.

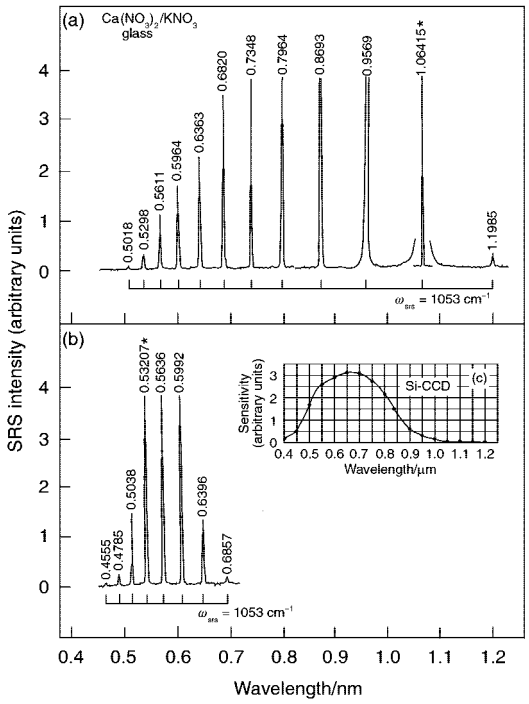

Fig. 4 Room temperature single-pass laser Raman generation spectra of a ~10 mm long glassy $Ca(NO_3)_2:KNO_3=40:60$ (mol%) sample obtained under picosecond pumping at (a) $\lambda_{f1}=1.06415$ and (b) $\lambda_{f2}=0.53207$ μm fundamental wavelengths (indicated by an asterisk). The Stokes and anti-Stokes lines due to the $[NO_3]^-$ ions SRS-active vibration mode of $\omega_{SRS}=1053\ cm^{-1}$ are indicated by brackets. Intensities of the Raman generation components and excitation lines are shown without a correction for the spectral sensitivity of the analysing system used (c).

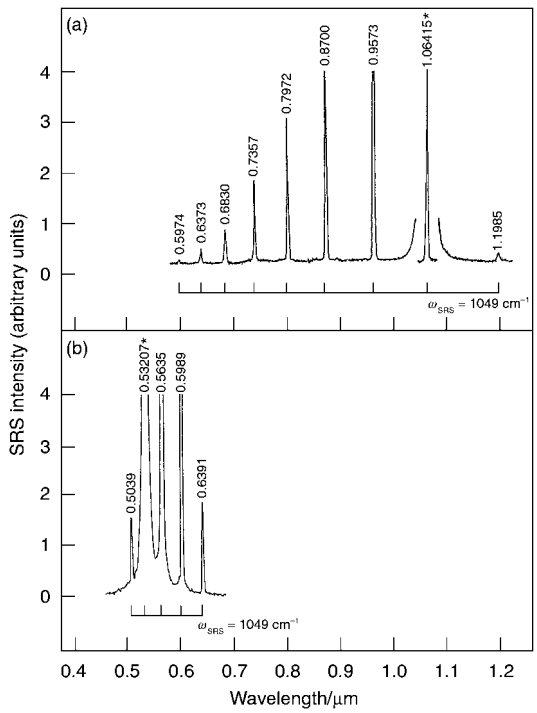

Fig. 5 Room temperature single-pass laser Raman generation spectra of a ~20 mm long glassy $Ca(NO_3)_2:Cd(NO_3)_2:KNO_3=29.11:15.62:55.27$ (mol%) sample obtained under picosecond pumping at (a) $\lambda_{f1}=1.06415$ and (b) $\lambda_{f2}=0.53207$ μm fundamental wavelengths (indicated by an asterisk). For further details, see Fig. 4.

CKN glasses, we used a one-micron $Nd^{3+}:Y_3Al_5O_{12}$ picosecond laser with a ~30% efficient external KTP frequency doubler generating ~110 ps (FWHM) pulses at a wavelength of $\lambda_{f1}=1.06415$ μm and an energy of up to 10 mJ, and ~80 ps SHG pulses at $\lambda_{f2}=0.53207$ μm. The laser beam with the λ_{f1} and λ_{f2} wavelengths providing a Gaussian spatial profile was focused into 10 mm long CKN (Fig. 4) and into 20 mm long composite (Fig. 5) glass samples with a lens ($F=250$ mm), resulting in a beam waist diameter of approximately 75 μm. The spectral composition of the Stokes and anti-Stokes generation lines was recorded with a spectrometric mulitchannel analyser (CSMA) on the base of a grating monochromator and a Si-CCD array sensor (Hamamatsu model S3923-1023Q). The visible and near-IR SRS spectra obtained, as well as the wavelength dependence of the sensitivity for the analysing system employed (insert in Fig. 4), are shown in Fig. 4 and 5. The spectral reflectivity of the monochromator grating is mainly responsible for the UV edge. Details on the conditions for SRS excitation are given elsewhere.[8,10–13]

The observed Stokes and anti-Stokes components of the CKN glass (containing no oxide glass fibers) are summarized in Table 1. Efficient $\chi^{(3)}$ nonlinear processes in the $Ca(NO_3)_2:KNO_3=40:60$ (mol%) material converted the fundamental pump radiation at $\lambda_{f1}=1.06415$ μm into the visible up to the 10th anti-Stokes emission with $\lambda_{ASt_{10}}=0.5018$ μm [Fig. 4(a)]. Stokes lines are not visible because of the spectral limit of the Si detector. The SRS conversion efficiency in 10 mm long samples (inside a cuvette) into all the Stokes and anti-Stokes lines under steady-state excitation ($\tau_p \gg T_2=1/\pi\Delta\nu_R$, with one micron pumping power density of approximately 1 GW cm^{-2}) reached about 30%. T_2 is the dephasing time and $\Delta\nu_R \approx 14\ cm^{-1}$ is the linewidth of the corresponding Raman-shifted line in the spontaneous Raman scattering spectra (Fig. 3).

The observed Stokes and anti-Stokes components of the composite glass are summarised in Table 2. Efficient $\chi^{(3)}$ nonlinear processes in the $Ca(NO_3)_2:Cd(NO_3)_2:KNO_3=29.11:15.62:55.27$ (mol%) material converted the fundamental pump radiation at $\lambda_{f1}=1.06415$ μm into the visible up to the 7th anti-Stokes emission with $\lambda_{Ast_7}=0.5974$ μm [Fig. 5(a), Stokes lines are not visible because of the spectral limit of the Si detector]. For Stokes lines, see Fig. 4(b) and 5(b).

Table 1 Spectral composition of the multiple Stokes and anti-Stokes generation in glassy $Ca(NO_3)_2:KNO_3=40:60$ (mol%) at 300 K under picosecond $Nd^{3+}:Y_3Al_5O_{12}$ laser pumping at $\lambda_{f1}=1.06415$ (upper part) and $\lambda_{f2}=0.53207$ μm (SHG, lower part) wavelengths

Stokes and anti-Stokes generation component SRS and RFWM line assignment

Line	Wavelength[a]/μm	Assignment
ASt_{10}	0.5018	$\omega_{f1}+10\omega_{SRS}$
ASt_9	0.5298	$\omega_{f1}+9\omega_{SRS}$
ASt_8	0.5611	$\omega_{f1}+8\omega_{SRS}$
ASt_7	0.5964	$\omega_{f1}+7\omega_{SRS}$
ASt_6	0.6363	$\omega_{f1}+6\omega_{SRS}$
ASt_5	0.6820	$\omega_{f1}+5\omega_{SRS}$
ASt_4	0.7348	$\omega_{f1}+4\omega_{SRS}$
ASt_3	0.7964	$\omega_{f1}+3\omega_{SRS}$
ASt_2	0.8693	$\omega_{f1}+2\omega_{SRS}$
ASt_1	0.9569	$\omega_{f1}+\omega_{SRS}$
λ_{f1}	1.06415	ω_{f1}
St_1	1.1985	$\omega_{f1}-\omega_{SRS}$
ASt_3	0.4555	$\omega_{f2}+3\omega_{SRS}$
ASt_2	0.4785	$\omega_{f2}+2\omega_{SRS}$
ASt_1	0.5038	$\omega_{f2}+\omega_{SRS}$
λ_{f2}	0.53207	ω_{f2}
St_1	0.5636	$\omega_{f2}-\omega_{SRS}$
St_2	0.5992	$\omega_{f2}-2\omega_{SRS}$
St_3	0.6396	$\omega_{f2}-3\omega_{SRS}$
St_4	0.6857	$\omega_{f2}-4\omega_{SRS}$

[a]Measurement accuracy is ±0.0003 μm.

Table 2 Spectral composition of the multiple Stokes and anti-Stokes generation in glassy $Ca(NO_3)_2 : Cd(NO_3)_2 : KNO_3 = 29.11 : 15.62 : 55.27$ (mol%) at 300 K under picosecond $Nd^{3+} : Y_3Al_5O_{12}$ laser pumping at $\lambda_{f1} = 1.06415$ (upper part) and $\lambda_{f2} = 0.53207$ μm (SHG, lower part) wavelengths

Stokes and anti-Stokes generation components SRS and RFWM line assignment

Line	Wavelength[a]/μm	Assignment
ASt_7	0.5974	$\omega_{f1} + 7\omega_{SRS}$
ASt_6	0.6373	$\omega_{f1} + 6\omega_{SRS}$
ASt_5	0.6830	$\omega_{f1} + 5\omega_{SRS}$
ASt_4	0.7357	$\omega_{f1} + 4\omega_{SRS}$
ASt_3	0.7972	$\omega_{f1} + 3\omega_{SRS}$
ASt_2	0.8700	$\omega_{f1} + 2\omega_{SRS}$
ASt_1	0.9573	$\omega_{f1} + \omega_{SRS}$
λ_{f1}	1.06415	ω_{f1}
St_1	1.1979	$\omega_{f1} - \omega_{SRS}$
ASt_1	0.5039	$\omega_{f2} + \omega_{SRS}$
λ_{f2}	0.53207	ω_{f2}
St_1	0.5635	$\omega_{f2} - \omega_{SRS}$
St_2	0.5989	$\omega_{f2} - 2\omega_{SRS}$
St_3	0.6391	$\omega_{f2} - 3\omega_{SRS}$

[a]Measurement accuracy is ±0.0003 μm.

4 Summary

We have demonstrated efficient multiple Stokes and anti-Stokes generation by SRS in a nitrate glass. The optical vibration mode $\omega_{SRS} = 1053\ cm^{-1}$ resulted in anti-Stokes generation up to the 10th line at $\lambda_{ASt_{10}} = 0.5018$ μm. The nitrate glasses show comparable SRS properties as do crystals of $Sr(NO_3)_2$ and $Cs(NO_3)$.[8]

Nitrate glasses were mechanically stabilised by the incorporation of oxide glass fibers, which allowed crack-free 20 mm long samples to be obtained in cuvettes. Due to a residual mismatch of the refractive indices, the composite glass showed some scattering of laser light. This accounts for the fact that anti-Stokes generation was observed only to the 7th line at $\lambda_{ASt_7} = 0.5974$ μm.

We have given a similar analysis of the SRS properties of polyphosphate glass, $(NaPO_3)_x$ in a previous publication.[40] The first review of this subject, covering many crystalline materials, was published during the preparation of this article.[41]

Acknowledgements

This work is supported by the Swiss National Science Foundation (project: 7SUPJ062279.00/1). A. A. K. wishes to acknowledge partial financial support by the Russian foundation for Basic Research and the State Scientific Programs "Fundamental Metrology" and "Fundamental Spectroscopy". We thank Dr Jean-Nicolas Aebischer (École d'Ingénieurs et d'Architectes de Fribourg), A. Devaux (University of Berne) for carrying out spontaneous Raman scattering experiments, and G. M. A. Gad for his help with the SRS measurements. The authors acknowledge cooperation within the Joint Open Laboratory for Laser Crystals and Precise Laser Systems.

References

1 W. Kaiser and M. Maier, in *Laser Handbook*, ed. F. T. Arrichi and E. O. Schulz-Dubois, North-Holland, Amsterdam, 1972, vol. 2.
2 J. T. Murray, R. C. Powell and N. Peyghambarian, *J. Luminesc.*, 1996, **66–67**, 89.
3 Yu. N. Polivanov, *Usp. Fizol. Nauk (Moscow)*, 1974, **126**, 185.
4 A. A. Kaminskii, H. J. Eichler, K. Ueda, N. V. Klassen, B. S. Redkin, L. E. Li, J. Findeisen, D. Jaque, J. García-Sole, J. Fernández and R. Balda, *Appl. Opt.*, 1999, **38**, 4533.
5 W. D. Johnston, I. P. Kaminov and J. G. Bergman, *Appl. Phys. Lett.*, 1968, **13**, 190.
6 E. O. Ammann and C. C. Decker, *J. Appl. Phys.*, 1977, **48**, 1973.
7 A. S. Eremenko, S. N. Karpukhin and A. I. Stepanov, *Sov. J. Quantum Electron.*, 1980, **10**, 113.
8 A. A. Kaminskii, J. Hulliger, H. Eichler, J. Hanuza, J. Findeisen and P. Egger, *Dokl. Phys.*, 1999, **44**, 69.
9 K. Andryunas, Yu. Vishchakas, V. Kobelka, I. A. Mochalov, A. A. Pavlyuk and G. T. Petrovskii, *Zh. Eksp. Teor. Fiz., Pis'ma Red.*, 1985, **42**, 333.
10 A. A. Kaminskii, A. V. Butashin, H.-J. Eichler, D. Grebe, R. Macdonald, K. Ueda, H. Nishioka, W. Odajima, M. Tateno, J. Song, M. Musha, S. N. Bagaev and A. A. Pavlyuk, *Opt. Mater.*, 1997, **7**, 59.
11 J. Findeisen, H. J. Eichler and A. A. Kaminskii, *IEEE J. Quantum Electron.*, 1999, **35**, 173.
12 P. Franz, P. Egger, J. Hulliger, J. Findeisen, A. A. Kaminskii and H. J. Eichler, *Phys. Status Solidi B*, 1998, **210**, 7.
13 A. A. Kaminskii, S. N. Bagayev, J. Hulliger, H. Eichler, J. Findeisen and R. Macdonald, *Appl. Phys. B*, 1998, **67**, 157.
14 A. A. Kaminskii, A. V. Butashin, H. J. Eichler, D. Grebe, R. Macdonald, J. Findeisen, S. N. Bagayev, A. A. Pavlyuk, G. Aka, D. Vivien and D. Pelenc, *J. Raman Spectrosc.*, 1998, **29**, 645.
15 A. A. Kaminskii, S. N. Bagaev, A. M. Yurkin, A. E. Kokh, H. J. Eichler and J. Findeisen, *Dokl. Phys.*, 1999, **44**, 495.
16 A. A. Kaminskii, H. J. Eichler, K. Ueda, P. Reiche and G. M. A. Gad, *Quantum Electron.*, 2000, **30**, 1035.
17 A. A. Kaminskii, in *Raman Scattering—70 Years of Research*, ed. V. I. Gorelik, Lebedev Phys. Institute, Moscow, 1998, p. 206.
18 P. G. Zverev, J. T. Murray, R. C. Powell, R. J. Reeves and T. T. Basiev, *Opt. Commun.*, 1993, **97**, 59.
19 C. He and T. H. Chyba, *Opt. Commun.*, 1997, **135**, 273.
20 V. A. Berenberg, S. N. Karpukhin and I. V. Mochalov, *Sov. J. Quantum Electron.*, 1987, **17**, 1178.
21 K. A. Stankov and G. Marowsky, *Appl. Phys. B*, 1995, **61**, 213.
22 J. Findeisen, J. Hulliger, A. A. Kaminskii, H. J. Eichler, R. Macdonald, P. Franz and P. Peuser, *Phys. Status Solidi A*, 1999, **172**, 5.
23 J. T. Murray, W. L. Austin and R. C. Powell, in: *OSA TOPS, Vol. 19, Advances in Solid-State Lasers*, ed. V. R. Bosenberg and M. M. Fejer, Optical Society of America, Washington DC, 1998, p. 129.
24 A. A. Kaminskii, C. L. McCray, H. R. Lee, S. W. Lee, D. A. Temple, T. H. Chyba, W. D. Marsh, J. C. Barnes, A. N. Annanenkov, V. D. Legun, H. J. Eichler, G. M. A. Gad and K. Ueda, *Opt. Commun.*, 2000, **183**, 277.
25 R. H. Stolen and C. Lin, in *Handbook of Laser Science and Technology, Supplement 1*, CRC Press, Boca Raton, FL, 1991, p. 101.
26 K. Suzuki, K. Nogichi and N. Uesugi, *Opt. Lett.*, 1986, **11**, 656.
27 E. M. Dianov, P. V. Mamyshev, A. M. Prokhorov and V. N. Sekin, *Nonlinear Effects in Optical Fibers*, Harwood Academic Publishers, New York, 1989.
28 E. M. Dianov (ed.), *Proc. SPIE-Int. Soc. Opt. Eng.*, 2000, **4083**.
29 A. A. Kaminskii, N. S. Ustimenko, A. V. Gulin, S. N. Bagaev and A. A. Pavlyuk, *Dokl. Phys.*, 1998, **43**, 148.
30 G. A. Pasmanik, *Laser Focus World*, 1999, **35**, 137.
31 N. S. Ustimenko and A. V. Gulin, *Instrum. Exp. Tech. (Engl. Transl.)*, 1998, **41**, 386.
32 A. P. Rostkowsky, *Zh. Russ. Fiz.-Khim. O-va*, 1930, **62**, 2055.
33 E. Thilo, C. Wieker and W. Wieker, *Silikattechnik*, 1964, **15**, 109.
34 E. E. Vinogradow, I. A. Kirilenko, Y. I. Krasilov, V. G. Lebedev, V. F. Ryurikov, A. F. Solokha and G. V. Éllert, *Inorg. Mater.*, 1970, **6**, 1678.
35 H. Z. Cummins, G. Li, W. M. Du X. K. Chen, N. J. Tao and A. Saki, *AIP Conf. Proc.*, 1992, **256** (*Slow Dyn. Condens. Matter*), 40.
36 F. D. Bloss, *An Introduction to the Methods of Optical Crystallography*, Saunders College Publishing, Philadelphia, PA, 1961, pp. 50–60.
37 L. M. Torell, *J. Chem. Phys.*, 1982, **76**, 3467.
38 R. E. Hester and K. Krishnan, *J. Chem. Soc. A*, 1968, 1955.
39 S. C. Wait, Jr, A. T. Ward and G. J. Janz, *J. Chem. Phys.*, 1966, **45**, 133.
40 R. Burkhalter, B. Trusch, A. Kaminskii, G. M. A. Gad, H. J. Eichler and J. Hulliger, *Adv. Mater.*, 2001, **13**, 814.
41 J. Hulliger, A. A. Kaminskii and H. J. Eichler, *Adv. Funct. Mater.*, 2001, **11**, 243.